



Published in final edited form as:

*J Control Release*. 2010 June 1; 144(2): 233–241. doi:10.1016/j.jconrel.2010.02.006.

## Formulation, Characterization and Pulmonary Deposition of Nebulized Celecoxib Encapsulated Nanostructured Lipid Carriers

Ram R. Patlolla<sup>1</sup>, Mahavir Chougule<sup>1</sup>, Apurva R. Patel<sup>1</sup>, Tanise Jackson<sup>1</sup>, Prasad NV Tata<sup>2</sup>, and Mandip Singh<sup>1,\*</sup>

<sup>1</sup>College of Pharmacy and Pharmaceutical Sciences, Florida A&M University, Tallahassee, FL 32307, USA. Tel: 850-561-2790; Fax: 850-599-3813

<sup>2</sup>Division of Clinical Pharmacology, Covidien/Mallinckrodt, Inc., St. Louis, MO 63042

### Abstract

The aim of the current study was to encapsulate celecoxib (Cxb) in the Nanostructured Lipid Carrier (Cxb-NLC) nanoparticles and evaluate the lung disposition of nanoparticles following nebulization in Balb/c mice. Cxb-NLC nanoparticles were prepared with Cxb, Compritol, Miglyol and sodium taurocholate using high-pressure homogenization. Cxb-NLC nanoparticles were characterized for physical and aerosol properties. In-vitro cytotoxicity studies were performed with A549 cells. The lung deposition and pharmacokinetic parameters of Cxb-NLC and Cxb solution (Cxb-Soln) formulations were determined using Inexpose™ system and Pari LC star jet nebulizer. The particle size and entrapment efficiency of Cxb-NLC formulation were  $217 \pm 20$  nm and  $> 90\%$ , respectively. The Cxb-NLC released the drug in controlled fashion, and in vitro aerosolization of Cxb-NLC formulation showed FPF of  $75.6 \pm 4.6\%$ , MMAD of  $1.6 \pm 0.13$   $\mu\text{m}$  and GSD of  $1.2 \pm 0.21$ . Cxb-NLC showed dose and time dependent cytotoxicity against A549 cells. Nebulization of Cxb-NLC demonstrated 4 fold higher  $\text{AUC}_{0-24}$  in lung tissues compared to Cxb-Soln. The systemic clearance of Cxb-NLC was slower (0.93 L/h) compared to Cxb-Soln (20.03 L/h). Cxb encapsulated NLC were found to be stable and aerodynamic properties were within the respirable limits. Aerosolization of Cxb-NLC improved the Cxb pulmonary bioavailability compared to solution formulation which will potentially lead to better patient compliance with minimal dosing intervals.

### Keywords

Inhalation; Nanostructured lipid carrier; Celecoxib; Lung cancer; Lung disposition

## 1. Introduction

Inhalation drug delivery represents a potential delivery route for the treatment of several pulmonary disorders. Inhalation drug delivery have several advantages over conventional (parenteral and oral) dosage forms such as a) non-invasive b) circumventing first pass metabolism and systemic toxicity c) reduced frequent dosing and d) the inhaled drug reaches directly to the lung epithelium thereby enhancing local drug concentrations. In pulmonary drug delivery systems, surfactants and co-solvents are often used to prepare stable formulations of

\*For editorial correspondence and reprint requests mandip.sachdeva@gmail.com.

**Publisher's Disclaimer:** This is a PDF file of an unedited manuscript that has been accepted for publication. As a service to our customers we are providing this early version of the manuscript. The manuscript will undergo copyediting, typesetting, and review of the resulting proof before it is published in its final citable form. Please note that during the production process errors may be discovered which could affect the content, and all legal disclaimers that apply to the journal pertain.

highly lipophilic active ingredients and inhalation of formulations utilizing excipients cause lung inflammation [1]. It is expected that encapsulation of lipophilic compounds in nanoparticles will improve the stability by protecting the active ingredient from degradation and release the encapsulated drug in controlled manner for prolonged period of time [2]. Among several inhalation drug delivery systems, biodegradable nanoparticles have demonstrated several advantages in terms of protecting the active ingredient from degradation and releasing the drug in controlled manner for prolonged periods of time. Although few attempts have been made to deliver anticancer agents using nanoparticles and liposomes via inhalation route, the major limitations of these systems are instability during nebulization, biodegradability, drug leakage and associated drug adverse side effects [3,4]. Solid lipid nanoparticles (SLN) have several advantages such as a) good tolerability, b) biodegradability and c) greater stability against the shear forces generated during nebulization [3,5] compared to polymeric nanoparticles [3], liposomes [4] and emulsions [6]. SLN are produced by replacing the oil lipid of an o/w emulsion with a solid lipid or a blend of solid lipids, where the lipid particle matrix being solid at both room and body temperature. Despite greater stability, SLN have some limitations such as low drug loading, risk of gelation and drug leakage during storage caused by lipid polymorphism [7]. Therefore, in order to decrease the degree of organization of lipid matrix in SLN and increase the drug loading capacity, the nanostructured lipid carriers (NLC) have been developed and reported as the second generation of lipid nanoparticles. NLC nanoparticles are comprised of inner oil core surrounded by outer solid shell and hence allow the high payload of a lipophilic drug [8]. NLC nanoparticles have been investigated for topical delivery of lipophilic anti-inflammatory molecules and also in the cosmetic products [9,10].

Cyclooxygenase-2 (COX-2) enzyme is over-expressed among various human malignancies and is thought to have a potential role in the pathogenesis of non small cell lung cancer (NSCLC) [11]. Celecoxib (Cxb), a lipophilic COX-2 inhibitor has shown synergistic anticancer activity in combination with other anticancer agents such as docetaxel [11]. The preclinical data suggest that the COX-2/prostaglandin E2 signaling pathway plays an essential role in conferring the malignant phenotype in non-small cell lung cancer by stimulating angiogenesis, inhibiting apoptosis and suppressing the immune response. It has been also shown that Cxb inhibits NF- $\kappa$ B activation through inhibition of IKK and Akt activation which leads to down-regulation of COX-2 synthesis and other genes needed for inflammation, proliferation, and carcinogenesis [12]. In lung cancer patients, Cxb is also known to inhibit the overproduction of prostaglandin E2, as well as modulate the IL-10 production in the lung microenvironment [13]. Cxb is a poorly water soluble drug (7  $\mu$ g/ml) with a partition coefficient of 3.68 [14] and necessitates use of surfactants and co-solvent such as ethanol to formulate an aerosol formulation. Our earlier studies showed that Cxb formulations prepared using tocopheryl polyethylene glycol succinate and ethanol resulted in improved solubility and enhanced the anticancer activity of nebulized Cxb [15-16]. However, these formulations were un-stable and precipitation was observed on long term storage. Therefore, it is expected that encapsulation of Cxb in NLC nanoparticles will improve the stability and alter its pharmacokinetics by enhanced retention [17] and releasing the Cxb in a controlled fashion.

In the present investigation, we explored the feasibility of NLC nanoparticles as a novel carrier system for inhalation drug delivery of Cxb. Therefore in this study, we examined the effect of Cxb-NLC on the release of Cxb, aerodynamic properties and in-vitro cytotoxicity against A549 NSCLC cells. The present investigation was also aimed to evaluate the in vivo pulmonary deposition and systemic availability of aerosolized Cxb loaded NLC (Cxb-NLC) nanoparticles in Balb/c mice utilizing Inexpose® exposure chamber.

## 2. Material and Methods

### 2.1. Materials

Cxb was a generous gift from Pfizer (Skokie, IL). The triglyceride Miglyol 812 was obtained from Sasol Germany GmbH (Witten, Germany) and Compritol® 888 ATO was a kind gift sample from Gattefosse (Saint Priest, France). Taurocholic acid sodium salt was procured from Sigma-Aldrich Chemicals (St. Louis, MO). Dialysis tubing (Molecular weight Cut off: 6000-8000 Daltons and flat width of 23 mm) was obtained from Fisher Scientific (Pittsburg, PA). Polyoxyethylene-20 oleyl ether or Volpo-20 (Oleth-20) was a kind gift from Croda Inc (New Jersey, USA). Vivaspin centrifuge filters (Molecular weight Cut off: 10, 000 Daltons) was procured from Sartorius Ltd, (Stonehouse, UK). Fetal bovine serum (FBS), antibiotics and DID-oil (a lipophilic fluorescent dye with excitation 644 nm, emission 665 nm) were procured from Invitrogen Corp (Eugene, OR). The A549 human NSCLC cell line was obtained from American Type Culture Collection (Rockville, MD, USA). A549 cells were grown in F12K medium (Sigma, St. Louis, MO, USA) supplemented with 10% FBS. All tissue culture media contained antibiotic antimycotic solution of penicillin (5000 U/ml), streptomycin (0.1 mg/ml), and neomycin (0.2 mg/ml). The cells were maintained at 37°C in the presence of 5% CO<sub>2</sub> in air. All other chemicals used in this research were of analytical grade.

### 2.2. Animals

Male Balb/c mice (20-25 g; Charles River Laboratories) were utilized for the studies. The protocol for *in-vivo* experiments was approved by the Animal Care and Use Committee, Florida A & M University. The animals were acclimated to laboratory conditions for one week prior to experiments and were on standard animal chow and water *ad libitum*. The temperature of room was maintained at 22 ± 1 °C and the relative humidity of the experimentation room was found in the range of 35–50 %. For nebulization studies, prior to 4-5 days start of experiment animals were trained by nebulizing water for 30 min. This is to acclimated the nebulization environment and prevent any discomfort during the formulation nebulization.

### 2.3. Nanoparticle Preparation

A Cxb-NLC formulation was prepared by hot melt homogenization technique [9]. In brief, 0.02 % w/w of Cxb was dissolved in dichloromethane and mixed with lipid phase comprised of Compritol (7.0 % w/w) and Miglyol (3.0% w/w). Later, organic phase was removed on a rota evaporator for 2-3 h at 80 °C and to the heated lipid phase the aqueous solution (40 ml) containing sodium taurocholate (1.5% w/w) surfactant was added at same temperature under high speed mixing using a Cyclone IQ2 with Sentry™ Microprocessor (USA) at 20,000 rpm for 1 min. The resultant oil-in-water dispersion was passed through Emulsiflex-C5 (Avestin, Ottawa, Canada) high-pressure homogenizer at 5000 psi for 5 cycles. Throughout the process temperature was maintained at 80 °C. The Cxb-NLC and placebo NLC (without Cxb) formulations were prepared for comparison.

### 2.4. Characterization of nanoparticles

The particle size of NLC nanoparticle formulation was measured using BI-90 particle sizer (Brookhaven Instruments, Boston, USA), which is based on the principle of Dynamic Light Scattering and Zeta potential measurement was carried with Zeta plus (Brookhaven Instruments). In order to verify the total amount of drug present in the system, 0.1 ml of Cxb-NLC formulation was dissolved in 0.9 ml of tetrahydrofuran and subsequent dilutions were made with acetonitrile. Prior to HPLC analysis for Cxb content, samples were centrifuged at 13,000 rpm for 15 min and 100 µl of supernatant was injected into HPLC. Entrapment efficiency was determined using vivaspin centrifuge filters as per reported method [18]. In brief, Cxb-NLC (0.5 ml) formulation was placed on top of the vivaspin centrifuge filter

membrane (molecular weight cut-off 10,000 Daltons) and centrifuged at 3500 rpm for 15 min. The aqueous phase collected at the bottom of vivaspin filter membrane was subjected to high-performance liquid chromatography (HPLC) analysis to determine the Cxb content. To determine the drug loading, 1.0 ml of Cxb-NLC formulation was centrifuged at 16,000 g for 1.5 h and the pellet was dissolved in tetrahydrofuran. The amount of Cxb present in the pellet was estimated by HPLC. Drug loading was calculated based on the amount of Cxb identified in a measured amount of NLC using following equation [19]

$$\text{Drug Content (\%w/w)} = (\text{mass of Cxb in NLC} \times 100) / (\text{mass of NLC recovered}) \quad (1)$$

## 2.5. Differential Scanning Calorimetry

The interaction of Cxb with lipids and association of Cxb in NLC nanoparticle formulation was determined using a DSCQ100 (TA instrument, DE). Approximately 10 mg of formulation was weighed into an aluminium pan and sealed hermetically, and the thermal behavior was determined in the range of 10 to 225 °C at a heating rate of 5 °C·min<sup>-1</sup>. Baselines were determined using an empty pan, and all the thermograms were baseline-corrected. Transition temperatures were determined from the endothermic peak minima while transition enthalpies were obtained by integration of the endothermic transitions using linear baselines.

## 2.6. In-vitro drug release studies

In vitro drug release studies were conducted with a cellulose membrane (6000-8000 molecular weight cut off) using a USP 1 (basket) dissolution apparatus (Vankel, NC) for 72 h with the help of 900 ml of phosphate buffer saline (PBS) pH 7.4 containing 0.1% w/v Volpo-20 as dissolution medium. Cellulose membranes were soaked overnight in dissolution medium. To the pre-swollen cellulose membrane bags 2 ml of Cxb-NLC formulation was placed and both the ends of bags were tied to prevent any leakage. Later, dialysis bags were carefully placed in the baskets and the baskets were rotated at 50 rpm for 72 h at 37.0 ± 0.1 °C. As a control, 5 ml of saturated solution of Cxb prepared in 0.2% w/v Volpo-20 was placed in the dialysis bag and dialysis was carried in 75 ml of dissolution medium. At regular time intervals 1 ml of sample was collected and replaced with equal volume of dissolution medium. Amount of Cxb released in to the medium was determined with the help of HPLC analysis. The experiments were carried out in triplicate.

## 2.7. In-vitro aerosol characterization

Aerodynamic particle size distribution was measured using an 8-stage non viable, Anderson cascade impactor (Graseby-Andersen, Atlanta, GA, USA) equipped with filters on each stage and a backup filter. To prevent particle bounce during nebulization, each plate on the impactor was coated with 10 % w/v pluronic L10 in ethanol solution. The Cxb-NLC formulation was nebulized for 5 min into the cascade impactor operated at a flow rate of 28.3 L/min. After nebulization with Pari LC Star jet nebulizer, the amount of formulation deposited on throat, impactor stages (0-7) and filter was collected by washing with 5 ml of tetrahydrofuran and centrifuged at 13,000 rpm for 15 min. The amount of Cxb in the supernatant was analyzed using HPLC.

The mass median aerodynamic diameter (MMAD) and geometric standard deviation (GSD) were obtained from impactor data using Battelle software. The aerodynamic particle size distribution measurement is based on the amount of Cxb deposited on each stages of cascade impactor and represents a relative particle distribution. Percent throat deposition, respirable mass, and respirable fractions were calculated from the known amount of drug deposited on the various components. Only particles measuring less than 5 µm in diameter were included

in assessing the respirable mass and fraction. Impactor experiments were repeated at least three times.

The Droplet Size Distribution (DSD) measurement of Cxb-NLC formulation was also conducted by laser diffraction using a Malvern Spraytec<sup>®</sup> with RT Sizer Software. The Pari LC Star jet nebulizer filled with 3 ml of NLC formulation was nebulized at a flow rate of 28.3 L/min and aerosol was aspirated with the help of suction pump on the opposite side of the laser beam. The measurements were conducted at 3 cm from the laser beam and the focal length of the lens used was 100 mm, which has a droplet-size range of 0.5 – 200  $\mu\text{m}$ . The FPF values determined using a Malvern Spraytec<sup>®</sup> equipped with RT Sizer Software will represent the actual respirable fraction of a formulation.

## 2.8. In-vitro cytotoxicity studies

The in-vitro cytotoxicity of Cxb-NLC was evaluated in A549 cell line as reported earlier [20, 21]. For comparison Cxb-Soln for cell cytotoxicity studies was prepared by dissolving Cxb in dimethyl sulfoxide and subsequently diluted with cell culture medium. The final dimethyl sulfoxide concentration was less than 1% v/v in control and treatment groups [21]. The A549 cells were plated in 96-well micro titer plates, at a density of  $1 \times 10^6$  cells/well and after overnight incubation the cells were treated with various concentrations of Cxb-Soln and Cxb-NLC formulations diluted in F12K medium (20 to 320  $\mu\text{g}/\text{ml}$ ). The cells were incubated for 24, 48 and 72 h at  $37 \pm 0.2^\circ\text{C}$  in a 5%  $\text{CO}_2$ -jacketed incubator. The cell viability in each treatment at regular time intervals was determined using crystal violet assay. The percentage of cell survival as a function of drug concentration was then plotted to determine the  $\text{IC}_{50}$  value (the drug concentration needed to prevent cell proliferation by 50%).

## 2.9. Stability of Cxb - NLC during aerosolization

The in-vitro efficacy of aerosolized Cxb-NLC formulation was evaluated using a six-stage viable impactor using A549 cells [22,23]. To determine the amount of Cxb deposited on 4, 5 and 6 stages of viable impactor, petri plates filled with 15 ml of collection medium (PBS pH 7.4) were placed on each stage and Cxb-NLC formulation was nebulized for 2 min at a flow rate of 28.3 L/min. The Cxb-NLC deposited on each stage was extracted with 15 ml of tetrahydrofuran and the Cxb concentration in the solution was estimated using HPLC method. To ascertain the efficacy of aerosolized Cxb-NLC, similar type of experiment was carried out using viable impactor by placing a petri plate on stage 5 and the amount of free drug in the medium was collected using Vivaspin centrifuge filters and subjected to HPLC analysis.

## 2.10 In-vitro cytotoxicity of aerosolized Cxb-NLC against A549 Cells

To determine the in-vitro cytotoxicity of aerosolized Cxb-NLC formulation, the viable impactor was connected to the Pari LC Star jet nebulizer through an USP throat and operated at a flow rate of 28.3 L/min. A549 cells (one million in 15 ml of medium per petri plate) was plated in petri plates was placed on stage 5 of the viable impactor and exposed to the Cxb-NLC formulation for 2 min. After the exposure, the petri plate was taken out from the impactor, covered with sterile aluminum lids provided with the petri plate (Graseby Andersen, Smyrna, GA) and incubated at  $37^\circ\text{C}$  for 72 hours. Since all the operations were performed under biological safety cabinet (Class II, Type A/B3, NuAire, Inc., Plymouth, MN) using established tissue culture precautions, sterility can be maintained throughout the incubation period. At the end of incubation, the medium in the petri plate was discarded and the cells were rinsed three times with sterile PBS, and detached by adding trypsin. The cells were spun down with a centrifuge and resuspended in an appropriate amount of medium. The viable cells were then counted with a hemocytometer using trypan blue solution (0.4%). Untreated cells were used as control and for comparison cytotoxicity of Cxb was carried out by adding same amount of Cxb-Soln in to the petri plates.



### 2.11. In-vivo lung deposition and systemic pharmacokinetic studies

Inexpose™ (SCIREQ Scientific Respiratory Equipment Inc, Montreal, QC) system consisting of 12 ports located peripherally around a central delivery plenum was utilized for Cxb-NLC and ethanolic Cxb-Soln formulations aerosol exposure. For comparison, Cxb-Soln was prepared by dissolving Cxb in 100% ethanol to get a final concentration of 2 mg/ml. Aerosols were generated by nebulization with a Pari LC Star jet nebulizer using dry compressed air at a flow rate of 4.5 L/min. Male Balb/c mice ( $20 \pm 2$  g) were restrained in animal holders and placed in an inhalation chamber (SCIREQ, Montreal, Canada) such that only the nose of each mouse was exposed to the aerosol cloud. The nebulizer was connected to the top part of the inhalation chamber from which the generated aerosol flowed down the central tower to the peripherally arranged 12 mice. The total amount of  $23 \pm 3$  mg (Cxb-Soln) and  $9 \pm 2$  mg (Cxb-NLC) Cxb was nebulized to animals during 30 min exposure time. The total amount of Cxb deposited into each mouse was calculated based on the earlier reported method [16]. The estimated total deposited amount of inhaled Cxb (D) for the ambient air was calculated by the following formula

$$D=C \times V \times DI \times T \quad (2)$$

Where; C = concentration of Cxb in aerosol volume (163.60 µg/ml), V = volume of air inspired by the animal during 1 min [for mice, V = 1.0 L-min/kg], DI = estimated deposition index [fraction of inhaled dose deposited throughout the respiratory tract (for mice DI = 0.3)], T = Duration of treatment in min (T = 30 min).

After completion of the exposure, at predetermined time points (0, 0.5, 1, 2, 4, 6, 12 and 24 h) animals were sacrificed with overdose of halothane anesthesia. At each time interval six mice were sacrificed, blood and lungs were collected and samples were stored at - 80 °C until analyzed. Further to understand the lung deposition of NLC nanoparticles fluorescent dye encapsulated NLC (FI-NLC) nanoparticle was prepared by replacing the Cxb with DID-oil in the oil phase. The Balb/c mice were exposed to the FI-NLC nanoparticles for 30 min similar to Cxb-NLC formulation. The lungs were collected at 0.5 and 4 h of nebulization and processed as per reported method [21]. The tissue associated fluorescence was observed in the lung sections using Leica DM6000 inverted Laser Scan Confocal Microscope.

### 2.12. Plasma and Tissue Sample Analysis

100 µl plasma or lung tissue samples were spiked with 50 µl internal standard solution (100 µg/ml nimesulide in acetonitrile) and vortexed well. To the resultant samples 1.5 ml of dichloromethane was added, vortexed and then subjected to centrifugation (15 min at 3500 rpm) to separate aqueous and organic phases. The organic layer was separated, evaporated to dryness and the residue was then reconstituted with 200 µl of mobile phase and 100 µl was injected onto HPLC for quantification. In case of lung deposition studies, lungs were weighed and homogenized with 500 µl of phosphate buffered saline (pH 7.4) and processed similarly as that of plasma samples.

### 2.13. Celecoxib HPLC Bioanalytical method

The HPLC analysis of Cxb was performed as per reported method, with minor modifications [24]. Briefly, the method involves injection of plasma and tissue samples prepared as described above and resolved on HPLC system comprised of an auto sampler (model 717 plus), binary pump (model 1525), Waters UV photodiode array detector (model 996). The mobile phase consisting of acetonitrile, water, acetic acid (54:45:1% v/v) was pumped through the Symmetry C18 column (5 µm, 4.6 × 250 mm) at a flow rate of 1.0 ml/min and the eluent was monitored

at 254 nm. The Cxb stock solution was prepared with acetonitrile and the serial working standard solutions were prepared in mobile phase. Quantification of Cxb was accomplished by a calibration standard curve between 0.1 and 8 µg/ml using nimesulide as the internal standard and the calibration curve was found to be linear with  $r^2$  value of 0.996. Cxb extraction efficiencies from plasma and lung samples were  $86.8 \pm 9.3 \%$  and  $79.74 \pm 9.9 \%$  respectively.

#### 2.14. Pharmacokinetic and Statistical analysis

Routine pharmacokinetic parameters ( $C_{max}$ ,  $T_{max}$ , AUC and CLt) of Cxb in plasma and lung tissues were computed using non-compartmental approach (WinNonLin Version 5.2.1, Pharsight Corporation, Cary, NC). The plasma pharmacokinetics and lung deposition results were analyzed statistically using the Student's independent samples t test and expressed as one-way p value. When comparisons between groups yielded a value for  $p < 0.05$ , the difference between these groups was considered statistically significant. All statistical analyses were performed using the prism software.

### 3. Results and Discussion

#### 3.1. Nanoparticle Characterization

This is the first study which investigates the delivery of Cxb-NLC formulation for lung delivery. In the present study, we have used triglycerides such as Compritol and Miglyol to prepare the NLC nanoparticle formulation, where Compritol is a mixture of mono-, di- and triglycerides of behenic acid (C22) and form the solid outer shell of the nanoparticles. Miglyol (caprylic/capric triglycerides) is a liquid lipid, known to enhance the encapsulation of lipophilic drugs in the nanoparticles. Furthermore, addition of Miglyol to the Compritol tends to promote the formation of a small particle [25]. Development of inhalable nanoparticle formulations is quite challenging and in the present study we have prepared the Cxb-NLC formulation using triglycerides with a particle size of  $217 \pm 20$  nm and a polydispersity of 0.20. Particle size is one of the critical factor in aerosolization process, smaller the particle size more number of nanoparticles will accommodate into the micron size aerosol droplets and thereby enhance the delivery of drug to deep lung because of the increased diffusional mobility. Another advantage of smaller particle size is the rate of drug absorption increases by promoting more uniform drug distribution [26]. The zeta potential of placebo NLC and Cxb-NLC formulations in double distilled water (pH 6.4) was  $-27.38$  and  $-25.30$  mV, respectively. The total Cxb content assay results indicate that approximately 1.8 mg/ml of Cxb was present in the formulation. The entrapment efficiency (EE) and drug loading of Cxb-NLC formulation were 95.6 % and 4% w/w respectively. The liquid state of Miglyol oil helps to encapsulate the higher amount of drugs and reduces the particle crystallinity which imparts better stability and higher suitability for the controlled release [7].

#### 3.2. Differential Scanning Calorimetry

The DSC thermograms of Cxb, Compritol and physical mixture of Cxb with Compritol and Miglyol were represented in Fig. 1A. Cxb showed characteristic crystalline form melting peak at 162 °C and the physical mixture of Cxb and triglycerides show the disappearance of Cxb endothermic peak indicating that there is an interaction between the Cxb and lipid excipients (Fig. 1A). Furthermore, the thermal analysis of Cxb-NLC formulation also showed disappearance of sharp Cxb endothermic peak (Fig. 1B). The main advantage of NLC nanoparticle is presence of oil which helps to hold higher amount of drug and stabilize the nanoparticles.

The DSC thermogram of Compritol alone showed sharp endothermic peak at 69 °C, following addition of Miglyol and Cxb there was a depression in the endothermic peak mainly because these entities behave as impurities. Puglia et al [25] observed that addition of ketoprofen or

naproxen to the Compritol formulations resulted in the broadening of the Compritol endothermic peak. Similarly, DSC thermograms of Cxb-NLC showed broadening of Compritol peak and the reasons for this observation may be the excipients which undergo several heating and cooling cycles, the smaller size of the particles contributes larger surface area and also Miglyol, Cxb and surfactant may behave as impurities.

### 3.3. In-vitro release studies

In-vitro release of Cxb from NLC nanoparticle formulation was evaluated using USP dissolution apparatus, where the sink conditions were maintained using 900 ml of 0.1 % w/v Volpo-20 solution in PBS (pH 7.4) and the results are graphically represented in Fig. 2. In-vitro release studies are often carried out in a beaker or dissolution apparatus by directly placing nanoparticle formulations in the dissolution medium [24]. The limitations of these methods are improper stirring (beaker) and loss of formulation from the medium at each sampling time point (dissolution). To overcome these problems in the present study, nanoparticle formulation was securely placed in dialysis bags and in-vitro release studies were carried out with USP I dissolution apparatus at rotation speed of 50 rpm. Cxb is a lipophilic molecule and hence we have used 0.1 % w/v Volpo-20 in PBS as a dissolution medium. The saturation solubility of Cxb in 0.1, 0.2, 0.5 and 1% w/v Volpo-20 was 30, 60, 158 and 320  $\mu\text{g/ml}$ , respectively. The solubility of Cxb in Volpo-20 is several fold higher than with sodium lauryl sulfate (30  $\mu\text{g/ml}$  in 1% w/v), which is the most commonly used dissolution medium [24]. Kasting *et al* [27] observed that addition of Volpo-20 (1-6% w/v) to PBS increased the solubility of highly lipophilic capsaicin, vanillylnonanamide and olvanil compounds by several folds. The use of 0.1 % w/v Volpo-20 was sufficient to maintain the sink conditions. The release studies demonstrated that, at initial 8 h, Cxb-NLC formulation released 8-10 % of Cxb and after 24 h the release was 34 %. At the end of 72 h, total of  $3.05 \pm 0.11$  mg Cxb was released from 2 ml of Cxb-NLC formulation. Whereas with Cxb-Soln formulation,  $\geq 95$  % ( $278 \pm 5.14$   $\mu\text{g/ml}$ ) of Cxb was released at the end of 8 h indicating that cellulose membrane was not a limiting factor in the controlled release of Cxb from Cxb-NLC formulation (Fig. 2). In case of Cxb-Soln, release studies with lower volume (75 ml) of dissolution medium was used in order to maintain similar conditions to that of Cxb-NLC formulations and also to overcome the experimental problems. The zero order, first order and Higuchi equations are widely used in determining the release kinetics of lipid nanoparticles [28]. The release pattern of Cxb from Cxb-NLC follows zero order kinetics with a best fit  $r^2$  value of 0.99, where first order and Higuchi equations yield or best fit  $r^2$  value of 0.98 and 0.97 respectively. Overall, the Cxb-NLC formulation was able to release the Cxb in controlled manner and complete drug ( $> 80$  %) was released after 72 h (Fig. 2).

Similar observations were made by Zhang *et al* [29] where solid lipid microparticles prepared with Compritol showed slower clozapine release compared to microparticles made with tristearin mainly because of the distribution of clozapine in the inner area of the lipid matrix and has longer diffusion path length.

### 3.4. In-vitro aerosol characterization

To determine the aerodynamic behavior, freshly prepared Cxb-NLC formulation was nebulized with Anderson Mark-II cascade impactor. Cxb-NLC formulation showed FPF of  $75.6 \pm 4.6$  %, MMAD of  $1.6 \pm 0.13$   $\mu\text{m}$  and GSD of  $1.2 \pm 0.21$ . With Spraytec, the Cxb-NLC formulation showed  $Dv_{50}$  of 2.68  $\mu\text{m}$  with FPF of  $80.84 \pm 0.64$  % indicating that the aerodynamic values are well in agreement with that of cascade impactor values and more than 70 % of aerosolized nanoparticles were below 5  $\mu\text{m}$ . Particle size distribution is one of the important parameter in inhalation delivery, which determines the efficiency of the delivery system to deliver the particles deep enough to the alveolar region. Aerosol particles with aerodynamic diameter



between 1 and 3  $\mu\text{m}$  is optimal for inhalation drug delivery and these characteristics are suitable for pulmonary deposition throughout the respiratory zone [30].

### 3.5. In-vitro Cytotoxicity

The cytotoxicity of Cxb-NLC was determined against A549 NSCLC cells by incubating with various concentrations of formulation for 24, 48 and 72 h (Fig. 3). In-vitro cytotoxicity results showed a direct relation between Cxb concentration vs exposure time. After 24 h of exposure, the Cxb-Soln and Cxb-NLC showed the  $\text{IC}_{50}$  values of 78.75 ( $\pm 8.3$ ) and 252.02 ( $\pm 29.6$ )  $\mu\text{g/ml}$  respectively; with increase in exposure time to 48 h, the  $\text{IC}_{50}$  values decreased to 44.2 ( $\pm 2.6$ ) and 102.31 ( $\pm 5.4$ )  $\mu\text{g/ml}$  respectively. At 72 h, the  $\text{IC}_{50}$  values of Cxb-Soln and Cxb-NLC were 22.33 ( $\pm 0.78$ ) and 27.36 ( $\pm 2.2$ )  $\mu\text{g/ml}$  respectively. A strong correlation was observed between  $\text{IC}_{50}$  values and in-vitro release of Cxb-NLC formulation. The Cxb-NLC in-vitro release studies showed that approximately 35, 60 and 85% of Cxb was released at 24, 48 and 72 h and based on Cxb-NLC  $\text{IC}_{50}$  values the calculated amount of free drug available at 24, 48 and 72 h was 88.21 ( $\pm 10.4$ )  $\mu\text{g/ml}$ , 61.40 ( $\pm 3.3$ )  $\mu\text{g/ml}$  and 23.23 ( $\pm 1.86$ )  $\mu\text{g/ml}$  respectively (Table 1).

These results also suggest that in case of Cxb-NLC formulation, the Cxb was completely associated with the nanoparticles and released in a controlled manner over a period of 72 h. The blank NLC formulation had no effect on the cell viability and after 72 h of treatment with NLC nanoparticles, the cell viability was found to be  $\geq 90$ . The observed cytotoxicity with Cxb-NLC formulation was mainly because of i) the Cxb was released in controlled manner for prolonged period of time and/or ii) possibly due to cell internalization of nanoparticles over period of time. Our previous studies with monensin liposome formulation demonstrated that cell internalization of liposomes was time dependent and the particles were endocytosed slowly [31].

### 3.6. Stability and in-vitro cytotoxicity of aerosolized Cxb-NLC

Cxb dose deposited on stages 4, 5 and 6 of the viable impactor following 2 min nebulization of Cxb-NLC was 173 ( $\pm 29.56$ ), 373.43 ( $\pm 26.26$ ) and 101.51 ( $\pm 12.66$ )  $\mu\text{g}$ , respectively. It was observed that Cxb-NLC deposition was maximum on stage 5; hence we selected stage 5 for in-vitro cytotoxicity studies against A549 cells. Furthermore, aerosolization of Cxb-NLC formulation was found to be stable against shear stresses generated during nebulization with non-significant ( $p > 0.05$ ) change in particle size and loss of originally entrapped Cxb from NLC formulation. Aerosolization of Cxb-NLC for 2 min against A549 cells kept on stage 5 of the viable impactor inhibited the cell viability by 50.04% ( $\pm 1.49$ ). Incubation of A549 cells with 373.43  $\mu\text{g}$  of Cxb-Soln for 72 h showed 58.45% ( $\pm 1.69$ ) of cell viability inhibition and which was comparable with that of aerosolized Cxb-NLC.

### 3.7. Lung deposition of Cxb encapsulated NLC

To understand the lung deposition of nanoparticles, we collected the lungs at 5, 10, 20 and 30 min post nebulization and observed that following 20 min of exposure Cxb lung concentrations was found to be constant. However, after 30 min of exposure, a two fold increase in lung concentrations was observed (Fig. 4). According to our previous studies 30 min nebulization is adequate to deposit sufficient amount of Cxb in the lungs to elicit anticancer activity [16]; therefore in the present study, same protocol was adopted.

From equation 2, the calculated amount of Cxb deposited following 30 min nebulization of Cxb-NLC and Cxb-Soln was 1.47 and 4.82 mg/kg, respectively. The dose variation between Cxb-Soln and Cxb-NLC might be due to the differences in the density of solid content in respective formulations. Because of these differences aerosolization of Cxb-Soln produce droplet (fine mist) which will hold more amount of Cxb content compared to aerosolized Cxb-

NLC droplets, where later case the formulation contain the uniformly suspended lipid particles which will have higher density than the ethanolic solution. Fig. 5 represents the percent of Cxb dose deposited per lung tissue following nebulization of Cxb-Soln and Cxb-NLC formulations. After 30 min of Cxb-Soln and Cxb-NLC nebulization, the percentage of Cxb deposited in the lungs was 84.48 and 78.4 percent of Cxb dose per lung tissue, respectively. It was observed that with Cxb-Soln, the Cxb lung clearance was faster and after 6 h of nebulization, the Cxb lung concentrations fell to 4.9 percent of Cxb administered dose and at 12 h the Cxb lung concentrations was below detection limit (Table 2; Fig. 5). In contrast, Cxb-NLC formulation enhanced Cxb lung residence time by maintaining the Cxb concentration constantly for 2 h, followed by slow elimination and above detection limit for 12 h after inhalation (Fig. 5). A similar observation was made with FI-NLC nanoparticle where fluorescence was visualized after 4 h of inhalation in the lungs (Fig. 6). After 24 h of nebulization the Cxb-NLC was no longer detectable in the lung, which could be possibly due to mucociliary and macrophage clearance. However, the improved lung disposition of Cxb-NLC formulation was mainly attributed to the formulation composition and particle size. Schurch et al. [32] reported that mucus clearance could be overcome by nanoparticles, possibly due to rapid displacement of particles to the airway epithelium via surface energetics. In case of Cxb-NLC, the outer surface of NLC is composed of lipophilic triglyceride, such as Compritol and hence there is more probability of nanoparticles adsorption to the surface of airway epithelium and overcome the mucociliary lung transit. The NLC clearance by macrophages is very less because of small particle size. Lauweryns and Baert [33] also demonstrated that particles of less than 260 nm can escape macrophage lung clearance. Furthermore, the controlled release of Cxb from Cxb-NLC formulation can be explained as Compritol is a mixture of long-chain fatty acid behenic acid (C22) with a low pulmonary toxicity [34] and known to degrade slowly compared to shorter chain length fatty acids. Muller et al [35] demonstrated that the degradation of three fatty acids is in the order of myristic acid, C14 (Dynasan 114) > Palmitic acid, C16 (Cetylpalmitate) > behenic acid (Compritol). However, when Cxb-NLC formulation was prepared with Dynasan 114, the encapsulation efficiency was less than 60 % and phase separation was observed (unpublished observation). Compritol has higher transition temperature and might be able to accommodate the Miglyol oil well enough within the nanoparticles. Encapsulation of Cxb in the NLC nanoparticle modulated the lung disposition of the Cxb, where the  $AUC_{t/D}$  of Cxb-NLC formulation was 4 fold higher than that of Cxb-Soln (Table 2).

### 3.8. Plasma Pharmacokinetics

Cxb disposition in the lung and plasma following exposure to Cxb-NLC and Cxb-Soln formulations was studied using non-compartmental analysis (WinNonlin 5.2.1, Pharsight Corporation). Encapsulation of Cxb in the NLC nanoparticle modulated the pharmacokinetic behavior of Cxb; the Cxb-NLC formulation showed significantly higher Cxb plasma levels at all time points and was detected in plasma for upto 24 h (Fig. 7). Despite initial higher lung deposition, the Cxb-Soln formulation showed lower plasma concentrations and the blood concentrations fell below detection limits after 6 h of nebulization. However, with Cxb-NLC formulation, the peak plasma concentrations were reached after 4 h of nebulization and thereafter the plasma Cxb concentration declined slowly. In case of Cxb-Soln formulation, the peak plasma concentration reached in 1.4 h and after that declined rapidly (Fig. 7). Pharmacokinetic parameters presented in the table 2 demonstrate the advantage of Cxb-NLC compared to Cxb-Soln formulation by inhalational route. Systemic clearance of Cxb with NLC nanoparticle (0.93 L/h) formulation was slower than Cxb-Soln (20.03 L/h). Estimation of plasma area under curve of Cxb-NLC formulation also indicated that the bioavailability from NLC formulation was higher than that of solution formulations, (Table 2). Entry of Cxb into the blood stream will depend on the release of Cxb from the nanoparticles either by diffusion or degradation of the solid lipid core. The particle size, shape and ventilation parameters plays

vital role in lung deposition of nanoparticles. By reducing the particle size to below 500 nm the deposition increases in all regions of the lung mostly because of increased diffusion mobility [36,37]. Inhaled particles regardless of their surface characteristics will be submersed into the lining layer after their deposition in small airways and alveoli [38]. The alveolar surface covered with 10-20 nm thick surfactant layer is composed of over 90 % of phospholipids and 10% of proteins [39]. Once nanomaterials are deposited onto the lining of the respiratory tract, they first interact with the mucous layer within the airways or the surfactant-lining of alveolar region. The alveolar surfactants are amphiphilic in nature and have the ability to deplete or dissolve the lipids present on the nanoparticle surfaces in extracellular lung fluids and undergo chemical dissolution in situ. Another reason for improved plasma pharmacokinetics of Cxb-NLC is, generally the low molecular weight hydrophobic molecules are rapidly absorbed by passive diffusion from the lung epithelial membrane [40]. Furthermore, diffusion from alveoli region is much faster because the thin monolayer is made of broad and compact cells providing large surface area. Although, part of the nebulized formulation will deposit in the tracheobronchial airways, the absorption of drug molecules from this region is minimal because of thicker layer of epithelial cells (10-60  $\mu\text{m}$ ) and lower surface area [34]. Moreover, the presence of sodium taurocholate, a known permeation enhancer [41] in the formulation might also contribute to the increased plasma concentration of Cxb-NLC. The anticancer activity of aerosolized Cxb-NLC in A549 orthotopic lung cancer model using Nu/nu mice are in progress in our lab to investigate the efficacy of developed formulation.

#### 4. Conclusion

The lipophilic Cox-2 inhibitor, Cxb, was successfully encapsulated in the NLC nanoparticles using triglycerides such as Compritol and Miglyol 812. The particle size of the nanoparticles was  $217 \pm 20$  nm and DSC results shows that Cxb was associated with the nanoparticles. The Cxb-NLC formulation was able to release the Cxb in controlled manner for prolonged period of time and the aerodynamic diameter was within the nebulization limits. Most of the nebulized nanoparticles were able to deposit in the alveolar region of the mice lungs and also enhanced the Cxb lung residence time. The plasma samples analysis indicated the controlled release of Cxb from the Cxb-NLC formulation, where the Cxb plasma levels were maintained constant levels for 6 h after nebulization and in case of Cxb-Soln the plasma levels fell rapidly below detection limits after 6 h. These investigations present alternate drug delivery system for increasing the Cxb availability at site of action (lung) utilizing NLC nanoparticle methodology and also these studies provide schematic presentation of the benefits of NLC nanoparticle providing higher retention and release. The exposure and clearance pattern observed between the lung and blood compartments are reflected in a similar pattern between the two test formulations.

#### Acknowledgments

We thank Ruth Didier, College of Medicine, Florida State University Tallahassee for her kind help in Confocal Microscopy studies.

#### References

1. Walker JE Jr, Odden AR, Jeyaseelan S, Zhang P, Bagby GJ, Nelson S, Happel KI. Ethanol exposure impairs LPS-induced pulmonary LIX expression: alveolar epithelial cell dysfunction as a consequence of acute intoxication. *Alcohol Clin Exp Res* 2009;33:357–365. [PubMed: 19053978]
2. Mehnert W, Mader K. Solid lipid nanoparticles: production, characterization and applications. *Adv Drug Deliv Rev* 2001;47:165–196. [PubMed: 11311991]
3. Hitzman CJ, Elmquist WF, Wattenberg LW, Wiedmann TS. Development of a respirable, sustained release microcarrier for 5-fluorouracil I: In vitro assessment of liposomes, microspheres, and lipid coated nanoparticles. *J Pharm Sci* 2006;95:1114–1126. [PubMed: 16570302]

4. Chougule M, Padhi B, Misra A. Nano-liposomal dry powder inhaler of amiloride hydrochloride. *J Nanosci Nanotechnol* 2006;6:3001–9. [PubMed: 17048511]
5. Videira MA, Botelho MF, Santos AC, Gouveia LF, DeLima JJ, Almeida AJ. Lymphatic uptake of pulmonary delivered radiolabelled solid lipid nanoparticles. *J Drug Target* 2002;10:607–613. [PubMed: 12683665]
6. Reddy PR, Venkateswarlu V. Pharmacokinetics and tissue distribution of etoposide delivered in long circulating parenteral emulsion. *J Drug Target* 2005;13:543–553. [PubMed: 16390815]
7. Müller RH, Radtke M, Wissing SA. Solid lipid nanoparticles (SLN) and nanostructured lipid carriers (NLC) in cosmetic and dermatological preparations. *Adv Drug Deliv Rev* 2002;54:S131–S155. [PubMed: 12460720]
8. Muller RH, Radtke M, Wissing SA. Nanostructured lipid matrices for improved microencapsulation of drugs. *Int J Pharm* 2002;242:121–128. [PubMed: 12176234]
9. Pardeike A, Hommoss A, Müller RH. Lipid nanoparticles (SLN, NLC) in cosmetic and pharmaceutical dermal products. *Int J Pharm* 2009;366:170–184. [PubMed: 18992314]
10. Joshi M, Patravale V. Nanostructured lipid carrier (NLC) based gel of celecoxib. *Int J Pharm* 2008;346(1-2):124–32. [PubMed: 17651933]
11. Hida T, Kozaki KI, Muramatsu H, Masuda A, Shimizu S, Mitsudomi T, Sugiura T, Ogawa M, Takahasi T. Cyclooxygenase-2 inhibitor induces apoptosis and enhances cytotoxicity of various anticancer agents in non-small cell lung cancer cell lines. *Clin Cancer Res* 2000;6:2006–2011. [PubMed: 10815926]
12. Shishodia S, Koul D, Aggarwal BB. Cyclooxygenase (COX)-2 inhibitor celecoxib abrogates TNF-induced NF- $\kappa$ B activation through inhibition of activation of I $\kappa$ B $\alpha$  kinase and Akt in human non-small cell lung carcinoma: correlation with suppression of COX-2 synthesis. *J Immunol* 2004;173:2011–22. [PubMed: 15265936]
13. Mao JT, Roth MD, Serio KJ, Baratelli F, Zhu L, Holmes EC, Strieter RM, Dubinett SM. Celecoxib modulates the capacity for prostaglandin E2 and interleukin-10 production in alveolar macrophages from active smokers. *Clin Cancer Res* 2003;9:5835–41. [PubMed: 14676104]
14. Seedher N, Bhatia S. Solubility Enhancement of Cox-2 Inhibitors Using Various Solvent Systems. *AAPS Pharm Sci Tech* 2003;4:E33.
15. Haynes A, Shaik MS, Chatterjee A, Singh M. Formulation and Evaluation of Aerosolized Celecoxib for the Treatment of Lung Cancer. *Pharm Res* 2005;22:427–439. [PubMed: 15835749]
16. Fulzele SV, Chatterjee A, Shaik MS, Jackson T, Singh M. Inhalation delivery and anti-tumor activity of celecoxib in human orthotopic non-small cell lung cancer xenograft model. *Pharm Res* 2006;23:2094–2106. [PubMed: 16902813]
17. Thakkar H, Sharma RK, Murthy RSR. Enhanced Retention of Celecoxib-Loaded Solid Lipid Nanoparticles after Intra-Articular Administration. *Drugs in R & D* 2007;8(5):275–285.
18. Patlolla RR, Vobalaboina V. Pharmacokinetics and tissue distribution of etoposide delivered in parenteral emulsion. *J Pharm Sci* 2005;94:437–445. [PubMed: 15614812]
19. Xiang QY, Wang MT, Chen F, Gong T, Jian YL, Zhang ZR, Huang Y. Lung-targeting delivery of dexamethasone acetate loaded solid lipid nanoparticles. *Arch Pharm Res* 2007;30(4):519–25. [PubMed: 17489370]
20. Jackson T, Chougule MB, Ichite N, Patlolla RR, Singh M. Antitumor activity of noscapiene in human non-small cell lung cancer xenograft model. *Cancer Chemother Pharmacol* 2008;63:117–126. [PubMed: 18338172]
21. Ichite N, Chougule MB, Jackson T, Fulzele SV, Safe S, Singh M. Enhancement of docetaxel anticancer activity by a novel diindolylmethane compound in human non-small cell lung cancer. *Clin Cancer Res* 2009;15:543–552. [PubMed: 19147759]
22. Cooney D, Kazantseva M, Hickey AJ. Development of a size-dependant aerosol deposition model utilizing airway epithelial cells for evaluating aerosol drug delivery. *Altern to Labor Animals* 2004;32:581–590.
23. Kazantseva, M.; Cooney, D.; Hickey, AJ. Development of a Lung Model Utilizing Human Alveolar Epithelial Cells for Evaluating Aerosol Drug Delivery. In: Byron, PR.; Dalby, RN.; Peart, J.; Farr, SJ., editors. *Respiratory Drug Delivery*. Vol. VIII. Davis Horwood International Publishing, Ltd.; Raleigh, NC, USA: 2002. p. 707-710.

24. Tan A, Simovic S, Davey KA, Rades T, Prestidge AC. Silica-Lipid hybrid (SLH) microcapsules: A novel oral delivery system for poorly soluble drugs. *J Control Rel* 2009;134:62–70.
25. Puglia C, Blasi P, Rizza L, Schoubben A, Bonina F, Rossi C, Ricci M. Lipid nanoparticles for prolonged topical delivery: an in vitro and in vivo investigation. *Int J Pharm* 2008;357:295–304. [PubMed: 18343059]
26. Yang W, Peters JI, Williams RO III. Inhaled nanoparticles--a current review. *Int J Pharm* 2008;356:239–47. [PubMed: 18358652]
27. Kasting GB, Francis WR, Bowman LA, Kinnett GO. Percutaneous Absorption of Vanilloids: In Vivo and in Vitro Studies. *J Pharm Sci* 1997;86:142–146. [PubMed: 9002474]
28. Venkateswarlu V, Manjunath K. Preparation, characterization and in vitro release kinetics of clozapine solid lipid nanoparticles. *J Control Release* 2004;24:627–638. [PubMed: 15023472]
29. Zhang L, Qian Y, Long C, Chen Y. Systematic Procedures for Formulation Design of Drug-Loaded Solid Lipid Microparticles: Selection of Carrier Material and Stabilizer. *Ind Eng Chem Res* 2004;47:6091–6100.
30. Byron PR. Prediction of drug residence times in regions of the human respiratory tract following aerosol inhalation. *J Pharm Sci* 1986;75:433–438. [PubMed: 3735078]
31. Singh M, Ferdous AJ, Jackson TL. Stealth monensin liposomes as a potentiator of adriamycin in cancer treatment. *J Control Rel* 1999;59:43–53.
32. Schurch S, Gehr P, Im Hof V, Geiser M, Green F. Surfactant displaces particles toward the epithelium in airways and alveoli. *Respir Physiol* 1990;80:17–32. [PubMed: 2367749]
33. Lauweryns JM, Baert JH. Alveolar clearance and the role of the pulmonary lymphatics. *Am Rev Respir Dis* 1977;115:625–683. [PubMed: 322558]
34. Sanna V, Kirschvink N, Gustin P, Gavini E, Roland I, Delattre L, Evrard B. Preparation and In Vivo Toxicity Study of Solid Lipid Microparticles as Carrier for Pulmonary Administration. *AAPS PharmSciTech* 2004;5:e27. [PubMed: 15760085]
35. Muller RH, Ruhl D, Runge AS. Biodegradation of solid lipid nanoparticles as a function of lipase incubation time. *Int J Pharm* 1996;144:115–121.
36. Byron PR, Patton JS. Drug delivery via the respiratory tract. *J Aerosol Med* 1994;7:49–75. [PubMed: 10147058]
37. Jaques PA, Kim CS. Measurement of total lung deposition of inhaled ultrafine particles in healthy men and women. *Inhal Toxicol* 2000;12:715–731. [PubMed: 10880153]
38. Geiser M, Schurch S, Gehr P. Influence of surface chemistry and topography of particles on their immersion into the lung's surface-lining layer. *J Appl Physiol* 2003;94:1793–1801. [PubMed: 12547838]
39. Goerke J. Pulmonary surfactant: functions and molecular composition. *Biochim Biophys Acta* 1998;1408:79–89. [PubMed: 9813251]
40. Patton JS, Byron PR. Inhaling medicines: delivering drugs to the body through the lungs. *Nat Rev Drug Discov* 2007;6:67–74. [PubMed: 17195033]
41. Kobayashi S, Kondo S, Juni K. Pulmonary delivery of salmon calcitonin dry powders containing absorption enhancers in rats. *Pharm Res* 1996;13:80–83. [PubMed: 8668684]



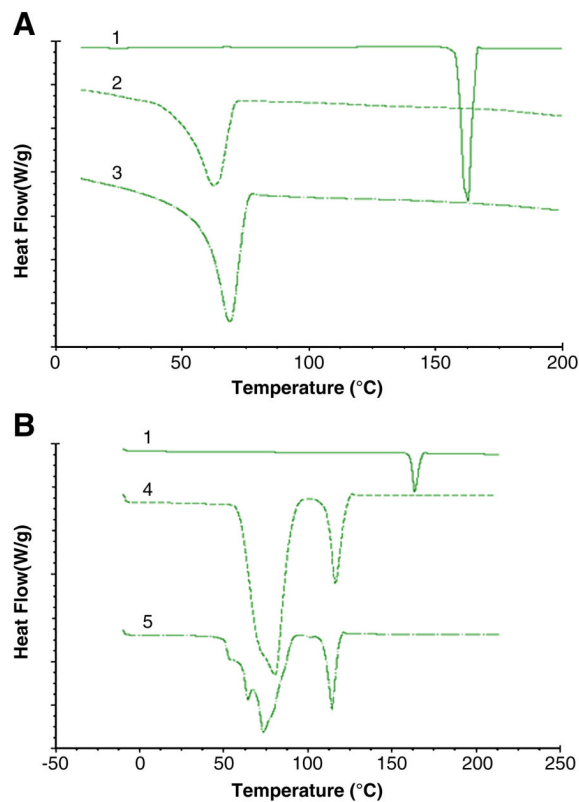


**Figure 1.** Differential Scanning Calorimetry of Cxb formulations. A) Cxb alone and in combination with the lipid excipients 1) Celecoxib pure drug 2) Compritol + Miglyol 3) Cxb-compritol physical mixture B) NLC formulation with and without Cxb, 4) blank NLC formulation 5) Cxb-NLC formulation.

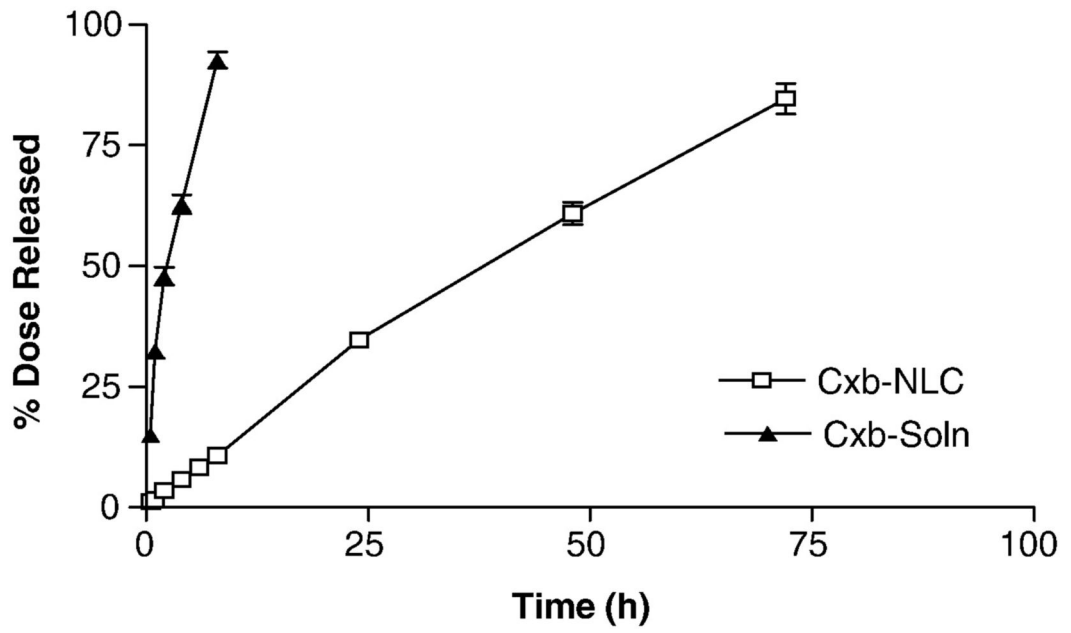


**Figure 2.**  
In-vitro drug release of Cxb from Cxb-Soln and Cxb-NLC formulations.

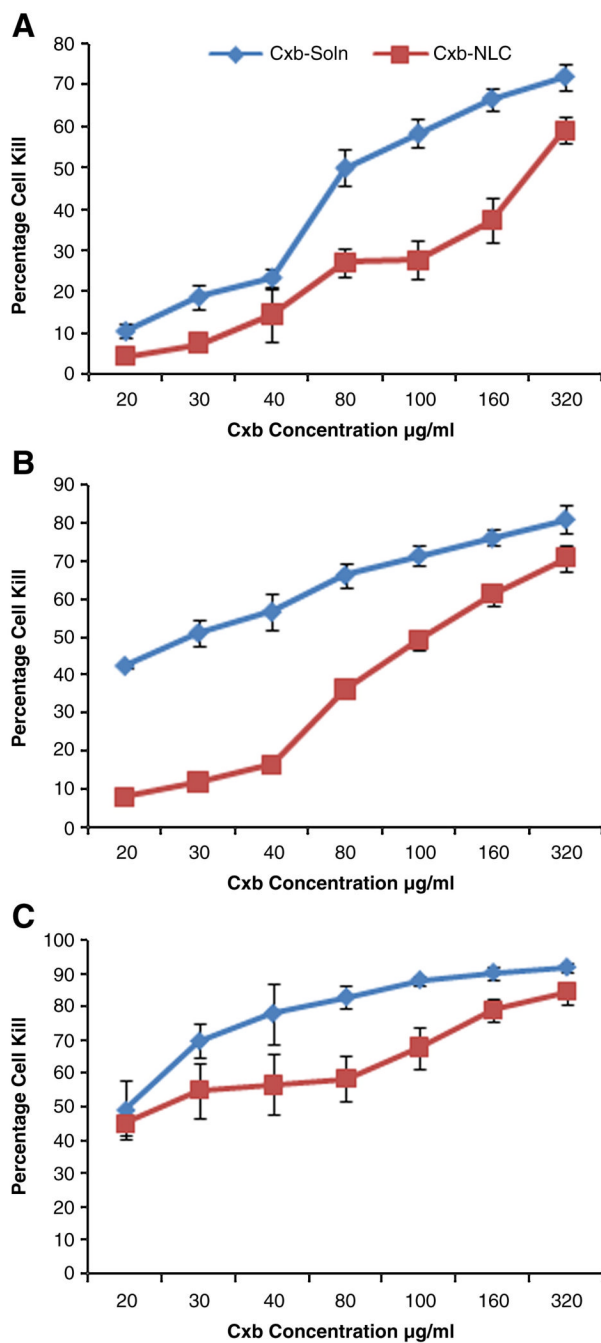


**Figure 3.** In-vitro cytotoxicity profile of Cxb-NLC formulation in A549 cells after A) 24 h B) 48 h C) 72 h of treatment. Cells were treated with various concentrations of Cxb-NLC and Cxb-Soln formulations and cytotoxicity was determined using crystal violet dye assay as described in Materials and Methods. A plot of the percentage of cell survival versus Cxb concentrations used for the determination of IC<sub>50</sub> values. Values represent the Mean ± SD of at least three separate determinations for each treatment group.

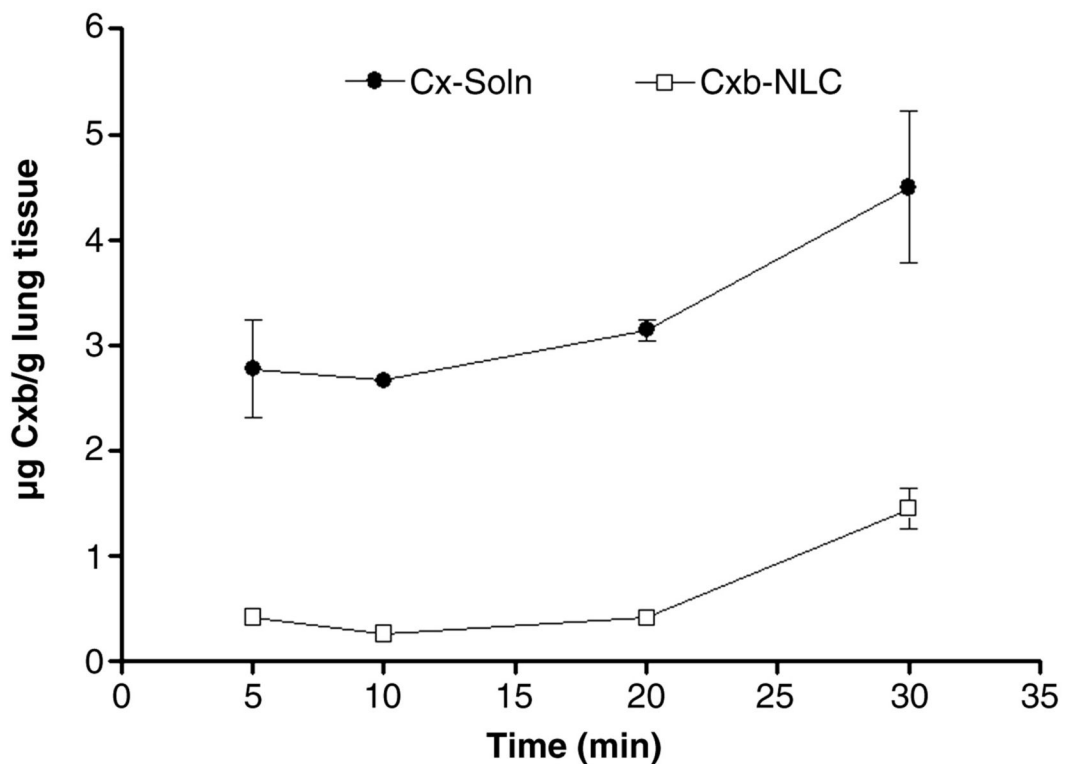


**Figure 4.** Effect of time on the lung deposition of Cxb-Soln and Cxb-NLC formulations. Following nebulization for 30 min, at regular time intervals 5, 10, 20 and 30 min the mice lungs were collected and the amount of Cxb deposited was determined using method as specified in the Materials and Methods section. The data represent the Mean  $\pm$  SD (n=6). ● Cxb-Soln and □ Cxb-NLC.

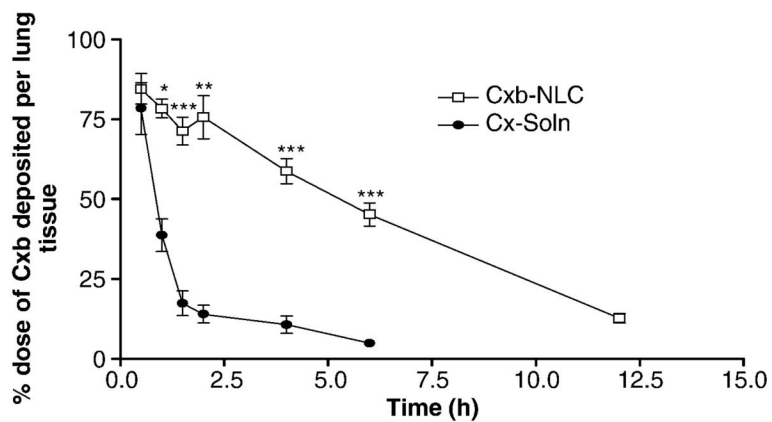


**Figure 5.** Lung deposition of Cxb-Soln and Cxb-NLC formulations after nebulization for 30 min using nose only Inexpose™ system and Pari LC Star jet nebulizer in Balb/c mice. The data represent the percent dose of Cxb deposited per lung tissue was plotted against time (Mean  $\pm$  SD), n=6.  
● Cxb-Soln and □ Cxb-NLC, \*p < 0.05; \*\*p < 0.01; \*\*\*p < 0.001.



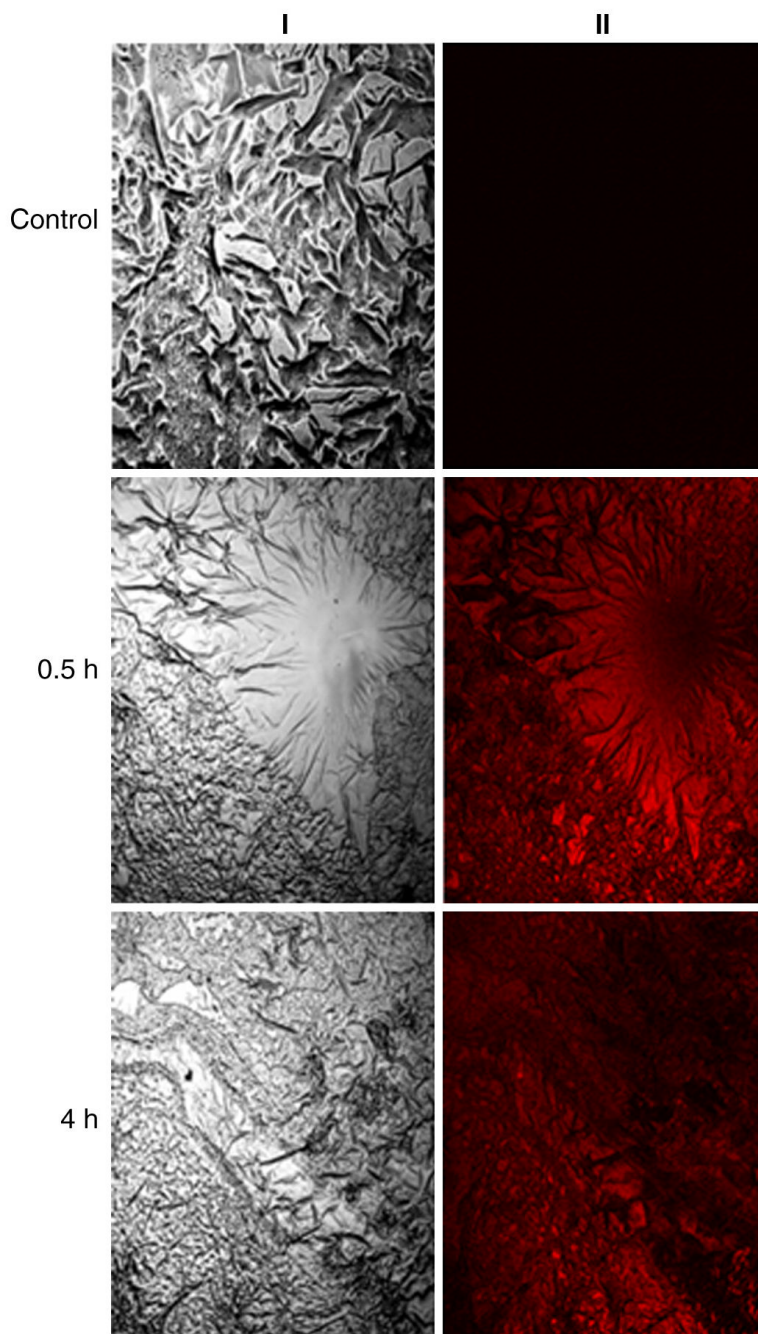


**Figure 6.** Lung disposition of DID-oil fluorescent dye loaded NLC (FI-NLC) formulation in Balb/c mice. FI-NLC formulation was nebulized to mice and the lungs were collected and processed for confocal microscopy as described in Methodology section. The fluorescent dye was visualized with confocal microscope. I) bright field II) fluorescent mode.

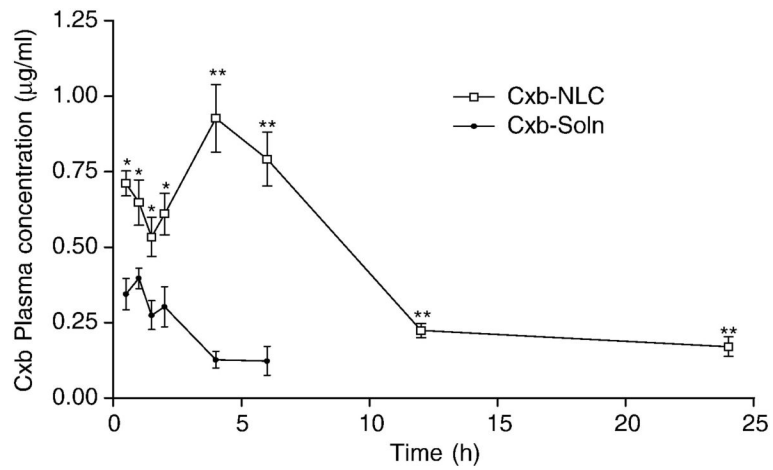


**Figure 7.** Plasma pharmacokinetics of Cxb-Soln and Cxb-NLC formulations after nebulization for 30 min using nose only Inexpose™ system and Pari LC Star jet nebulizer in Balb/c mice. ● Cxb-Soln and □ Cxb-NLC, \*p < 0.05; \*\*p < 0.01.

**Table 1**

In-vitro cytotoxicity of Cxb-Soln and Cxb-NLC formulations.

Time point (h)	IC50 values ( $\mu\text{g/ml}$ )		Cxb-NLC In-vitro release (%)	Cxb-NLC amount of Free Cxb available ( $\mu\text{g/ml}$ )
	Cxb-Soln	Cxb-NLC		
24	78.75 ( $\pm$ 8.3)	252.02 ( $\pm$ 29.6)	35	88.21 ( $\pm$ 10.4)
48	44.2 ( $\pm$ 2.6)	102.31 ( $\pm$ 5.4)	60	61.40 ( $\pm$ 3.3)
72	22.33 ( $\pm$ 0.78)	27.36 ( $\pm$ 2.2)	85	23.23 ( $\pm$ 1.86)

**Table 2**

Plasma pharmacokinetic and lung disposition parameters of Cxb-NLC and Cxb-soln following nebulization for 30 min in Balb/c mice.

Parameter	Plasma*		Lung**	
	Cxb-NLC	Cxb-soln	Cxb-NLC	Cxb-Soln
T <sub>max</sub> (h)	4.50 (22.2)	1.38 (54.5)	1.13 (66.7)	0.5 (0.0)
C <sub>max</sub> /D (µg/mL/mg)	0.11 (19.3)	0.02 (9.6)	0.21 (12.8)	0.23 (24.3)
AUC <sub>t</sub> /D	1.1 (4.8)	0.05 (15.82)	1.26 (14.6)	0.36 (9.8)
AUC <sub>inf</sub> /D	1.27 (10.5)	0.07 (15.4)	1.36 (16.1)	0.42 (6.6)
Cl (L kg/h)	0.93 (4.72)	20.03 (4.72)	0.81 (16.3)	27.77 (10.3)

^ data represent the Mean values (percent coefficient of variation); all the values are p < 0.05 is statistically significant difference with respect to Cxb-soln.

\* In case of plasma parameters units are T<sub>max</sub> time at which C<sub>max</sub> occurs (h), C<sub>max</sub> maximum concentration, AUC<sub>(t/D)</sub> total area under the curve (time zero to last measurable concentration, µg×hr /ml/mg), AUC<sub>inf/dose</sub> dose normalized total area under curve (time zero to infinity, µg×hr /ml/mg), Cl clearance.

\*\* Lung parameters units are expressed per g weight of the lung tissue e.g. C<sub>max</sub> is µg/g/mg dose, AUC<sub>(t/D)</sub> is µg×hr /ml/mg dose.